THE AMERICAN MINERALOGIST, VOL. 46, MAY–JUNE, 1961

DIFFRACTOMETER PATTERNS OF A.P.I. REFERENCE CLAY MINERALS

MARTIN W. MOLLOY AND PAUL F. KERR, *Columbia University, New York, N. Y.*

ABSTRACT

The widely used studies published by the American Petroleum Institute on reference clay minerals are supplemented by revised *x*-ray diffraction information based on the original specimens. Chemically analyzed samples of kaolinite, dickite, halloysite, nontronite, montmorillonite, illite, attapulgite and pyrophyllite are re-examined by recent *x*-ray diffractometer techniques. Spacing and intensity measurements and the corresponding diffractometer patterns are furnished for specimens oriented to enhance the basal reflections, subjected to glycolation and given 550° C. heat treatment. Constant instrument settings permit diffraction intensity comparison between different specimens, treatments, and species. The interpretation of the *x*-ray diffraction patterns in terms of the structural and thermal stability of the minerals is discussed.

INTRODUCTION

In 1950, cooperative studies of reference clay minerals, localities, and occurrence were published as reports on Research Project 49 of the American Petroleum Institute. Among the data presented were chemical analyses, electron micrographs, infra-red spectra, pH data, *x*-ray powder film measurements, semi-quantitative spectrographic analyses, base-exchange data, magnetic susceptibility, particle size determinations, optical measurements, and staining tests.

Since the publication of the A.P.I. studies there has been considerable development in the field of electronic devices for measuring the intensity and position of *x*-ray reflections. The convenience and accuracy of *x*-ray diffractometers in distinguishing and analyzing the clay minerals have led to the widespread use of diffractometer equipment in clay mineralogy. Visual recognition of the diffractometer pattern, together with profile characteristics such as peak amplitude, sharpness, and asymmetry are important improvements made possible by strip-chart recording. The facility with which structural changes such as lattice expansion and collapse may be observed, and even recorded continuously, has led to the replacement of film methods for many theoretical, and most routine, applications.

The data reported in A.P.I. Project 49 have frequently been quoted, and since the specimens were widely distributed numerous supplementary measurements have been published. In view of the scientific application the reference clay minerals have received, revised data on the original specimens should be of value. It is the purpose of this paper to give an improved sequence of *x*-ray diffractometer patterns and measurements on selected A.P.I. clay minerals uniformly applicable to the set as a

whole. In view of the widespread use of the technique of orienting clay mineral specimens to enhance basal x-ray reflections, it is of additional interest to furnish patterns and data of the reference clay standards oriented in this manner. Similarly, the employment of organic compounds to expand, and thereby distinguish the montmorillonite-type lattices, and the use of heat treatment to collapse the lattice of the kaolin group, are now common techniques for the analysis of clay minerals. Diffractometer patterns for the A.P.I. standards subjected to these treatments are also given, together with diffraction intensity and spacing measurements when these differ significantly from the untreated specimen.

The reference clay minerals studied include kaolinite, dickite, nonhydrated halloysite, nontronite, montmorillonite, illite, attapulgite and pyrophyllite. The particular minerals and specimens chosen were restricted to the chemically analyzed material. In most cases it was possible to study more than one specimen of a particular mineral, thus verifying the diffraction reflections which were obtained. In addition, the specimens of kaolinite yielded in their diffractometer patterns a representative range in crystallinity.

Clay minerals are rarely monomineralic or entirely free from impurities. While the American Petroleum Institute clay mineral set includes some of the most satisfactory reference clays which have been collected, it must be remembered that impurities were frequently noted in the original descriptions. It is possible by x-ray diffractometer techniques to identify impurities indicated by thermal, optical, or other techniques. Glycolation provides a method for recognition of small amounts of expanding-lattice, montmorillonoid minerals, and the interpretation of mixed-layer structures which were only theoretical possibilities at the time of the original A.P.I. study. Additional thermal, x-ray, and electron micrographic observations have increased knowledge of clay structures and the behavior of clay lattices during expansion and heat treatment. Similarly, the developments in mica polymorph studies during the past ten years have considerably clarified the illite problem.

In preparing the discussions and interpretations of the x-ray diffractometer patterns, the authors have drawn extensively from Brindley (1951), "The Identification and Structure of the Clay Minerals"; Grim (1953), "Clay Mineralogy"; and Mackenzie (1957), "The Differential Thermal Investigation of Clays." Many of the conclusions from the original American Petroleum Institute Research Project 49 report (Kerr *et al.*, 1951) have also been incorporated in the present paper.

This study has been carried on with the assistance of a graduate fellowship in geology awarded by the Union Carbide Ore Co., a division of the Union Carbide Corporation.

Instrumentation

A portion of the original A.P.I. specimen remaining after chemical analysis has been crushed, dispersed in distilled water, and sedimented onto glass slides. The entire specimen has been used, not merely the suspended fraction, so that the diffraction pattern represents the material used for chemical analysis.

An improved Norelco *x*-ray Diffractometer was used for the patterns after precise alignment and checking. The electronic circuit was equipped for pulse height analysis to reduce the background of hard radiation scatter. The patterns were completed within a short period to minimize the effect of equipment drift, and the instrument settings were maintained without change throughout this time.

The patterns were run with Ni filtered Cu radiation ($\lambda = 1.5418$ Å) at 40 kv, 17 ma potential, scanning speed of 1° 2θ per minute, with 1° and .003″ slits and a 17 cm. goniometer radius. Instrument settings of: scale factor 4, multiplier .6, time constant 4 sec., proportional counter voltage 1470 vdc, amplifier gain 50, base line 23 v, and channel width 11 v, were employed for all the patterns. The pulse height analyzer settings were chosen to discriminate in favor of Cu Kα radiation, sacrificing about 10 per cent of the initial intensity in the process, but supressing the background by a larger factor.

The scans were limited to the 4–60° 2θ range which corresponds to spacings from 22 to 1.55 angstroms. Three sedimented slides were prepared for each specimen by warm air drying. One was used as the untreated sample. A second was sprayed with a fine mist of diethylene glycol monobutyl ether until saturation, and then used as the glycolated specimen. The last slide was placed in an electric furnace at 550° C., $\pm 10°$ C., for two hours, and then slowly cooled.

The instrument settings were intentionally maintained constant throughout the examination of all specimens so that intensity measurements might be compared directly. The background reading was not subtracted from the measurements in order to eliminate this arbitrary factor. Two types of intensity measurements are presented, the relative (I_{REL}), and the absolute (I_{ABS}). The relative measurements given in per cent of the strongest reflection permit comparison with other published patterns, while the absolute intensities in units above the base allow comparison between different specimens, treatments, and species in this work. Thus the influence of admixed kaolinite upon the intensities in the diffractometer pattern of halloysite may be estimated, as well as the range in the degree of crystallinity among the kaolinites themselves.

The diffractometer patterns have been measured by direct overlay on a precise template reading in dÅ. The template aids the search for, and

determination of, minor or missing peaks, as well as the distinction of several overlapping patterns produced by the same specimen.

The chemical analyses of the A.P.I. specimens are given in Table I. Other data may be obtained by reference to the original descriptions (Kerr, *et al.*, 1951).

Kaolinite

X-ray diffractometer patterns of kaolinite (Fig. 1) are characterized by intense (001) and (002) reflections accompanied by a series of lesser peaks. Glycolation yields no noteworthy shift in the spacing or intensity of the peaks observed in the untreated pattern. Heating the specimens to 550° C. results in complete destruction of this pattern.

The number, intensity, and sharpness of the diffraction peaks recorded for a particular kaolinite sample depend primarily on the degree of crystallinity of the specimen. Brindley and Robinson (1946), and Murray and Lyons (1956) have presented studies showing the range in

TABLE I. CHEMICAL ANALYSES FOR AMERICAN PETROLEUM INSTITUTE REFERENCE CLAY MINERALS[1]

A.P.I. Number	Weight Per Cent														Per Cent Clay Mineral	Per Cent Impurity	TOTAL
	SiO_2	Al_2O_3	Fe_2O_3	FeO	MgO	CaO	Na_2O	K_2O	H_2O^+	H_2O^-	TiO_2	MnO	C	Other			
	Kaolinite $Al_4Si_4O_{10}(OH)_8$																
1a	45.48	38.84	0.19	--	0.17	0.24	0.24	0.42	13.66	0.71	0.86	--			97.19	2.81	100.81
8	45.11	37.02	1.24	0.17	0.11	0.22	0.36	0.71	13.44	0.80	1.30	--			93.26	6.74	100.48
9a	46.07	38.07	0.33	--	0.01	0.38	0.27	0.43	13.47	0.43	0.50	--	--	SO_3 Trace	96.39	3.61	99.96
10[2]																	
17	45.72	39.82	0.01	--	Trace	Trace	0.16	0.36	13.67	0.55	0.42	Trace	--		97.44	2.56	100.80
	Dickite $Al_4Si_4O_{10}(OH)_8$																
15a	43.95	39.72	--	0.01	Trace	0.84	0.12	0.52	14.59	0.10	0.02				94.43	5.57	99.89
15c	44.48	40.05	--	0.01	Trace	0.51	0.12	0.15	14.42	0.06	0.02				96.20	3.80	100.22
	Halloysite $Al_4Si_4O_{10}(OH)_8$																
14a	42.72	36.59	0.17	0.33	Trace	Trace	0.18	0.46	14.14	4.38	Trace	0.01	--		91.06	8.94	100.76
13	43.98	38.46	--	0.03	Trace	0.32	0.14	0.48	14.59	2.58	0.01				93.9	7.1	100.59
	Nontronite $Fe^{+3}_{2.00}(Al_{.33}Si_{3.67})O_{10}(OH)_2Na_{.33}$																
33a	40.54	5.19	31.24	0.39	0.06	1.92	0.14	0.24	6.00	14.75	--	--	--	Li_2O --			100.47
	Montmorillonite $(Al_{1.67}Mg_{.33})Si_4O_{10}(OH)_2Na_{.33}$																
19	50.95	16.54	1.36	0.26	4.65	2.26	0.17	0.47	8.28	15.01[4]	0.82	0.01	0.01				100.28
22	51.52	17.15	5.65	0.32	2.80	1.72	0.15	0.85	8.55	11.22	0.48	--					100.41
23	49.91	17.20	2.17	0.26	3.45	2.31	0.18	0.38	7.70	15.77	0.24	0.04	Trace	Li_2O --			99.47
27	58.53	19.61	3.10	0.13	2.65	0.25	1.68	0.31	6.21	7.89	0.12						100.48
28	51.69	18.65	4.08	0.23	1.64	0.24	0.08	0.17	7.89	14.82	0.16	--	--	CO_2 --			99.62
	Illite $(Al_{1.45}Fe_{.44}Mg_{.15})(Al_{.27}Si_{3.73})O_{10}(OH)_2(K, Ca)$																
35	56.91	18.50	4.99	0.26	2.07	1.59	0.43	5.10	5.98	2.86	0.81						99.50
36	57.41	17.96	4.99	0.26	2.25	0.64	0.15	5.75	6.70	2.97	0.82						99.90
	Attapulgite $Mg_5Si_8O_{20}(OH)_2 \cdot 8H_2O$																
44	53.96	8.56	3.10	0.19	10.07	2.01	0.03	0.39	11.51	9.79	0.24	--					99.85
	Pyrophyllite $Al_{2.00}Si_4O_{10}(OH)_2$																
47	77.43	16.51	0.47	--	0.05	0.41	0.22	1.26	22.87	0.11	0.18	--					99.51

[1] Kerr et al., Research Project 49, American Petroleum Institute, No. 7, pp. 43-45, 48-50, 52-55, 57-58 (1951)

[2] Ledoux & Company, Teaneck, New Jersey. Analysis #615328, A.P.I. No. 10 omitted in A.P.I. Research Project 49

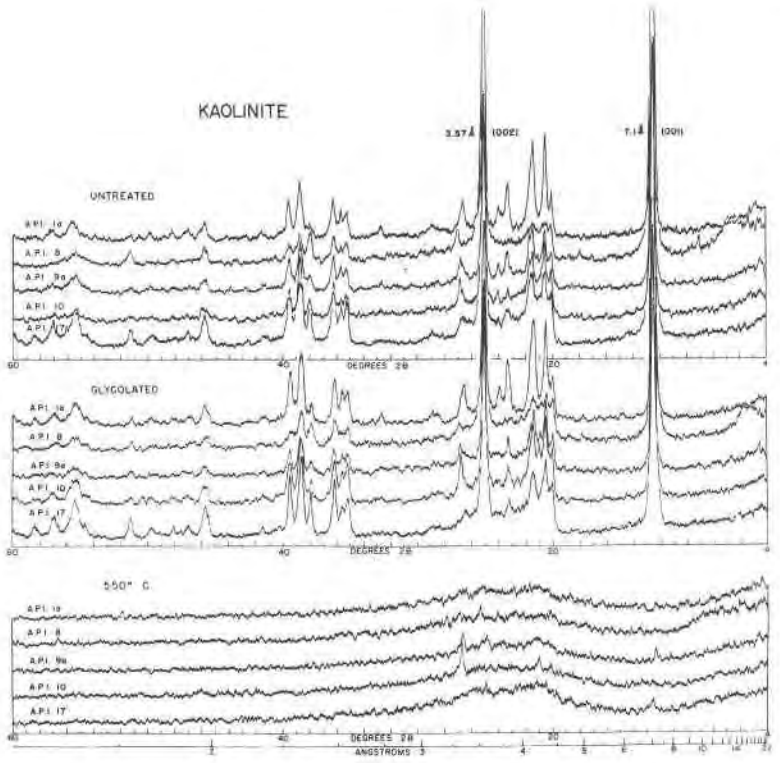

FIG. 1. X-ray diffractometer patterns of oriented A.P.I. Kaolinite.

crystallinity observed in kaolinites, and the gradual merging, broadening, and loss of diffraction lines with decrease in crystallinity. Similar effects may be noted by a comparison of measurements in Table II. In all cases, however, the (001) and (002) reflections at 7.1 and 3.58 Å, respectively, were recorded, together with groups of lines in the 4.5–3.6, 2.56–2.34, and 1.67–1.48 Å ranges.

The diffractometer pattern of the untreated sample is usually sufficient to distinguish kaolinite from other non-kaolin minerals. If the 14 Å (001) reflection of chlorite is not observed, the (003) reflection at 4.7 Å is usually present. Heating the sample to 550° C. will destroy the kaolinite pattern, leaving a chlorite pattern visible, together with other impurities which are thermally stable at that temperature. Montmorillonite is visible in the pattern of A.P.I. 8 (Fig. 1) with a small reflection at 14 Å which shifts to a larger spacing upon glycolation. Approximately 2 per cent quartz is responsible for the small, sharp peak recorded at 3.34Å in the heat treated pattern of A.P.I. 10.

TABLE II. X-RAY DIFFRACTOMETER SPACING AND INTENSITY MEASUREMENTS FOR ORIENTED A.P.I. KAOLINITE

KAOLINITE

Untreated

ASTM 5-0413[1]			A.P.I. 1a[2]			A.P.I. 8[3]			A.P.I. 9a[4]			A.P.I. 10[5]			A.P.I. 17[6]		
(hkl)	dA	I_{REL}	dA	I_{ABS}	I_{REL}	dA	I_{ABS}	I_{REL}	dA	I_{ABS}	I_{REL}	dA	I_{ABS}	I_{REL}	dA	I_{ABS}	I_{REL}
						(13.5-14.7)	25	20									
						(10.1)	18	14									
(001)	7.15	100	7.12	78	100	7.16	~132	100	7.13	~102	100	7.14	~108	100	7.13	~135	100
						(5.01)	11	8									
	4.45	50	4.44	23	29	4.44	21	16	4.45	20	20	4.44	24	22	4.44	26	19
	4.35	60	4.35	44	56	4.36B	21	16	4.38	29	28	4.34	30	28	4.35	34	25
	4.17	60	4.17B	42	54				4.17	30	29	4.16	35	32	4.17	32	24
						4.13B	21	16									
	4.12	30							4.12	26	25	4.12	31	29	4.13	32	24
	3.84	40	3.84	26	33				3.83B	20	20	3.83	17	16	3.83	19	14
	3.73	20	3.73	17	22				3.73	16	16	3.72	16	15	3.73	16	22
(002)	3.57	100	3.57	59	76	3.57	~114	87	3.57	71	68	3.57	79	73	3.57	~123	91
	3.37	40	3.37	20	26				3.35	19	19	3.37	17	16	3.37B	16	12
						3.30	21	16									
	3.14	20															
	3.09	20	3.09	11	14	3.09	13	10							3.09	11	8
	2.75	20	2.76	10	13				2.76	10	10						
	2.55	70	2.56	15	19	2.56	14	11	2.56	14	14	2.55B	15	14	2.55	22	16
	2.52	40	2.52	16	21	2.52	13	10	2.53	15	15	2.51	13	12	2.52	20	15
	2.486	80	2.48	20	26	2.49	17	13	2.49	19	19	2.48	16	15	2.49	29	22
(003)	2.374	70	2.38	11	14	2.38	18	14	2.39	12	12	2.37	13	12	2.38	23	17
	2.331	90	2.33	27	35	2.32	17	13	2.34	24	24	2.32B	20	18	2.33	39	29
	2.284	80	2.28	20	26	2.29	14	11	2.29	18	18	2.28	14	13	2.29	27	20
	2.243	5	2.24	8	10	2.23	9	7									
	2.182	30	2.17	9	12				2.18B	8	8				2.18B	9	7
	2.127	20	2.11	8	10	2.10B	8	6	2.11	7	7				2.12	8	6
						2.09	7	7									
	2.057	5	2.05	7	9												
	1.985	70	1.99	12	15	2.00B	13	10	1.99B	10	10	1.98B	10	9	1.99	17	13
	1.935	40	1.93	10	13				1.95	8	8				1.94	11	8
	1.892	20	1.89	9	12												
	1.865	5	1.87	7	9												
	1.835	40	1.82B	8	10				1.83	8	8				1.84	9	7
	1.805	5	1.80	7	9												
(004)	1.778	60	1.78	7	9	1.79	11	8	1.79	9	9	1.78	6	6	1.79	11	8
	1.704	5	1.70	7	9												
	1.682	10	1.68	11	14	1.68B	11	8	1.68	12	12	1.68	10	9	1.68B	19	14
	1.659	80	1.66B	12	15				1.67	11	11	1.66	7	6	1.67	13	10
	1.616	70	1.62B	9	12				1.62	9	9	1.62	7	6	1.62	15	11

[1] Unoriented specimen; Brindley and Robinson, Min. Mag., 27, 242-254 (1946).
[2] Unlayered; Murfreesboro, Arkansas. B = broad.
[3] Crude; Bath, South Carolina. Montmorillonite and halloysite reflections are enclosed in parentheses.
[4] White; Mesa Alta, New Mexico.
[5] Birch Pit, Macon, Georgia.
[6] Lewiston, Montana.

The distinction of kaolinite from other kaolin minerals is not as simple. Hydrated halloysite may be distinguished in the untreated pattern of A..I. 8 (Fig. 1) by the (001) spacing of 10.1 Å. However, non-hydrated halloysite, dickite, and nacrite yield patterns that are not greatly different from kaolinite.

Comparison of Figs. 1, 2, and 3 shows the principal similarities and differences between the *x*-ray diffractometer curves of kaolinite, dickite, and non-hydrated halloysite. The halloysite curve is far more diffuse than the curves for dickite or kaolinite, and the lattice spacings (Table

TABLE III. X-RAY DIFFRACTOMETER SPACING AND INTENSITY MEASUREMENTS FOR ORIENTED A. P. I. DICKITE

DICKITE								
Untreated								
ASTM 2-0104[1]			A. P. I. 15a[2]			A. P. I. 15c[3]		
(hkl)	dA	I_{REL}	dA	I_{ABS}	I_{REL}	dA	I_{ABS}	I_{REL}
(001)	7.2	100	7.17	~158	100	7.12	~163	100
	4.4	80	4.43	36	23	4.41	34	21
			4.24	18	11	4.25	21	13
	4.14	80	4.12	48	30	4.11	47	29
			3.93	16	10	3.93	16	10
	3.78	60	3.78	18	11	3.78	31	19
(002)	3.58	90	3.57	~145	92	3.58	~155	96
			3.48	18	11	3.48	15	9
	3.43	40	3.42	22	14	3.42	26	16
	3.27	20	3.24B	8	5	3.24B	8	5
	3.10	40	3.09	10	6	3.08B	9	6
						3.07	11	7
			3.04	14	9			
	2.93	40	2.92	13	8	2.92	15	9
	2.80	40				2.79	11	7
	2.56	70	2.56	15	10	2.56	19	12
	2.51	80	2.50	23	15	2.50	28	17
			2.42	26	16	2.42	14	9
(003)	2.39	60	2.38B	24	15	2.39	30	18
	2.33	90	2.32	36	23	2.31	49	30
			2.23	7	4			
	2.20	30	2.19B	10	6	2.19	12	7
			2.17	10	6	2.18B	11	7
	2.10	30	2.09	8	5			
			2.07	8	5			
	1.98	70	1.98	14	9	1.98	20	12
			1.94	11	7	1.94B	8	5
			1.92	9	5	1.92	6	4
	1.90	30	1.90	10	6	1.90	9	6
						1.88	9	6
	1.86	70	1.86	7	4	1.85B	7	4
(004)	1.79	60	1.79	14	9	1.79	17	11
			1.69B	10	6	1.68B	9	5
	1.65	80	1.66	11	7	1.65	20	12
			1.61B	8	5			
			1.59	7	4	1.59	7	4
	1.56	60	1.56B	9	5	1.56	12	7

[1] Unoriented specimen; Red Mountain, Colorado. McVay, L., and Thompson, J. Am. Cer. Soc., 11, 382 (1928): Gruner, J. W., Z. Krist, 83, 394 (1932): Nagelschmidt, G., Z. Krist., 87, 120 (1934).

[2] San Juanito, Chihuahua, Mexico. B = broad.

[3] San Juanito, Chihuahua, Mexico; different portion of pit.

IV) are somewhat larger than the corresponding spacings for the two other minerals (Tables II and III). Dickite, however, is somewhat similar to kaolinite in the number, spacing, sharpness, and intensity of the reflections. The main differences are in the larger number and increased sharpness of the dickite reflections, and in small changes in diffraction spacings. The dickite pattern, unlike kaolinite, persists upon careful heating to 550° C., the distinction between the two minerals being particularly apparent after heat treatment.

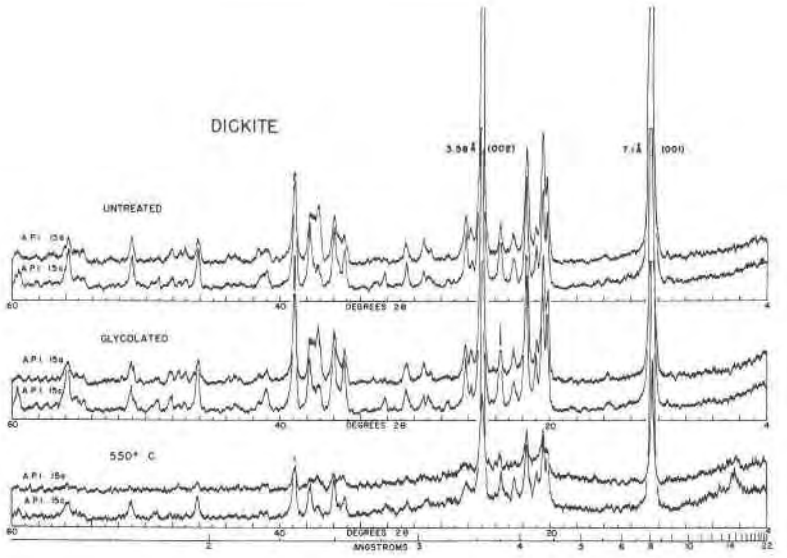

FIG. 2. *X*-ray diffractometer patterns of oriented A.P.I. dickite.

Differences in *x*-ray pattern and thermal behavior among the kaolin minerals are best revealed by reference to structural considerations. The basic structure common to the members of the group is that of kaolinite. This consists of a planar network of silica tetrahedra, joined at the base and with vertices pointing in the same direction. The vertices of the silica tetrahedra in turn are crosslinked in an octahedral pattern with aluminum and hydroxyl ions to form a stable, layer-like unit with a thickness of approximately 7 Å. Stacking these one-layer units above each other results in the kaolinite structure. The stacking pattern results in either a triclinic (kaolinite *T*) or pseudo-monoclinic (kaolinite p*M*) form. According to Gruner (1932), Ksanda and Barth (1935), and Hendricks (1938a), the dickite structure is formed by a stacking of two-layer units, and nacrite (Hendricks, 1938b) by a stacking of six-layer

kaolinite units. Thus, if the polymorph notation of Ramsdell (1947) is extended to kaolinite as proposed by Holdridge and Vaughn (Mackenzie, 1957, p. 98), then dickite would be kaolinite $2M$, and nacrite kaolinite $6M$.

Halloysite is apparently a kaolinite-like structure with considerable disorder in the arrangement, and perhaps also in the components, of the lattice. The mineral seems to be a species distinct from kaolinite as there is no intergradation known between the two. When fully hydrated, the halloysite lattice is thicker than kaolinite by approximately one layer of water. The resulting structure is asymmetric, curling to form long tubes. Upon dehydration the tubes often unroll and split, as seen in the excellent electron micrographs of Bates *et al.* (1950).

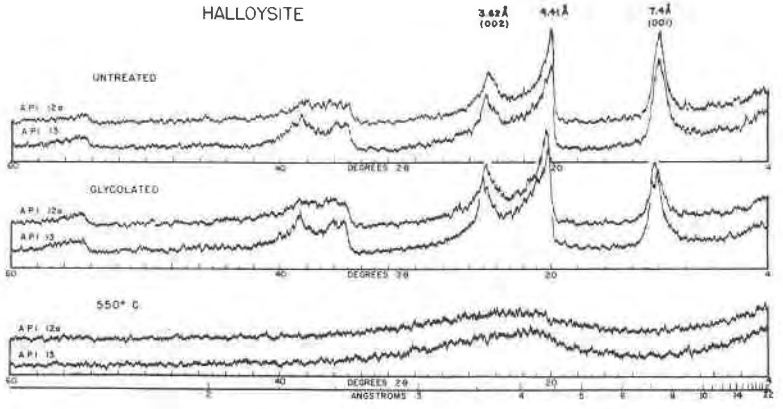

FIG. 3. *X*-ray diffractometer patterns for oriented, non-hydrated A.P.I. halloysite.

DICKITE

Dickite is a less common member of the kaolin group (Ross and Kerr, 1931), structurally similar to kaolinite, differing principally in the stacking of the layers.

The *x*-ray diffractometer patterns of dickite (Fig. 2) are distinguished by a series of sharp, intense reflections which are unaffected by glycolation, but reduced in intensity upon heating to 550° C. The two most intense peaks occur at 7.1 and 3.58 Å, representing, respectively, (001) and (002) reflections. Unlike kaolinite, where the diffraction pattern is destroyed at approximately 530° C., the pattern of dickite persists until above 600° C., at which point dehydration is complete. Differential thermal analysis records show dehydration as an endothermic reaction near 675° C., a considerably higher peak temperature than prevails

for other minerals of the kaolin group. This emphasizes the thermal stability of the dickite structure.

Electron micrographs show well-crystallized, euhedral plates with elongate hexagonal outlines, approximately 1–10 microns in diameter. Individual crystals of the mineral may be 1 mm. or more in diameter, sufficiently large to be easily visible to the unaided eye. Many smaller crystals are observable with an ordinary microscope, emphasizing excellent crystallinity, since the most ordered minerals usually give the largest crystals.

The two-layer unit cell of dickite is similar to the less common nacrite, a six-layer kaolinite structure, and the two are believed to be randomly and intimately intergrown in the San Juanito specimens (A.P.I. 15*a* and 15*c*). The diffraction patterns (Table II) indicate that the samples are otherwise pure, with quartz absent, and only a trace of chlorite in the 14 and 4.7 Å peaks of the heat treated A.P.I. 15*c* specimen.

Halloysite

The partly hydrated and fully hydrated forms of halloysite differ in the presence of a single molecular layer of water in the fully hydrated form. This results in an increase from the 7.4 Å (001) spacing of the non-hydrated form to 10.1 Å in hydrated halloysite.

The two specimens examined in this study were of the non-hydrated form, with an *x*-ray diffractometer pattern (Fig. 3) characterized by three weak, diffuse reflections at 7.4, 4.4 and 3.62 Å, and a series of smaller peaks in the 2.3–2.6 Å vicinity (Table IV). The diffuse diffraction pattern apparently results from considerable disorder in both the stacking and degree of hydration of the structural layers.

Although some workers have reported the formation of an organic-halloysite complex when the hydrated form is glycolated, there is no shift noted in the structural spacing of the non-hydrated specimens.

Heating halloysite to 550° C. results in a complete destruction of the *x*-ray diffractometer pattern (Fig. 3). This represents both the non-reversible loss of water from the hydrated form below 100° C., and the progressive loss of hydroxyl ions in octahedral coordination in the range from 400 to 500° C.

Nontronite

Nontronite is the iron-rich member of the montmorillonite group. Since the *x*-ray diffractometer patterns of nontronite summarize the behavior of the montmorillonite minerals, they are given first.

The few, diffuse reflections recorded for nontronite in Fig. 4 represent only (00*l*) and (*hk*0) spacings. The lack of crystallographic order in the

stacking of the layers causes the absence of true (*hkl*) reflections. The strongest peak, (001), ranges between 9.2 and 15.8 Å in the untreated specimen, depending upon the number of water layers, and the nature of the cations in the intersilicate position. Thus the lattice is of the "expandable" variety. The only other distinct reflection occurs at 4.5 Å and is about one half the intensity of the (001) peak (Table V). The intense background in the nontronite patterns is caused by fluorescence of iron under the copper radiation.

TABLE IV. X-RAY DIFFRACTOMETER SPACING AND INTENSITY MEASUREMENTS FOR ORIENTED, NON-HYDRATED A. P. I. HALLOYSITE

HALLOYSITE								
Untreated								
ASTM 2-0229[1]			A. P. I. 12a[2]			A. P. I. 13[3]		
(hkl)	dA	I_{REL}	dA	I_{ABS}	I_{REL}	dA	I_{ABS}	I_{REL}
(001)	7.48	60	7.4B	39	98	7.4B	39	100
	4.44	100	4.41B	40	100	4.42B	37	95
			4.34	28	70	4.34	32	82
(002)	3.62	40	3.62B	25	63	3.58B	26	67
	2.60	80	2.58B	12	30	2.57B	16	41
			2.52B	13	33	2.50-2.52	16	41
			2.49B	13	33			
(003)	2.33	80	2.32-2.39	14	35	2.33	19	49
						2.29B	16	41
			1.99	8	20			
	1.70	60	1.67-1.70	8	20	1.67-1.70	11	28
	1.64							

[1] Unoriented specimen; Toller Graben, Elbingerode, Harz, Germany. Nagelschmidt, G., Z. Krist., 87, 131 (1934).

[2] Blue; Bedford, Indiana. B = broad.

[3] Eureka, Utah.

Glycolation of the specimen results in the characteristic expansion of the lattice as the polar organic molecules orient themselves in the intersilicate position. The degree of expansion depends upon the particular organic molecule employed. Glycerol results in a (001) spacing of approximately 17.8 Å, while diethylene glycol monobutyl ether, employed in this study, caused an expansion to 15.4 Å. The 4.5 Å reflection is reduced slightly in intensity by the treatment, but does not shift in position.

Heat treatment of nontronite to 550° C. results in a decrease in the (001) spacing to approximately 9.6 Å; a decrease in the intensity of (001)

and 4.5 Å peaks; and the appearance of a strong, broad reflection at approximately 3.16 Å, probably corresponding to (003), a spacing which is not present in the untreated or glycolated structures. As this peak also appears in the heat treated patterns of montmorillonite, it is seemingly characteristic of the group. The 9.6 Å spacing represents the anhydrous nontronite structure after the loss of intersilicate water between 150–250° C., and partial loss of hydroxyl ions coordinated about Fe^{+3} ions in the octahedral position. The hydroxyl ions are not completely driven off until about 950° C., and the *x*-ray diffraction pattern persists until this point. The nature of the residual cations trapped in the intersilicate position after the loss of the H_2O with which they were

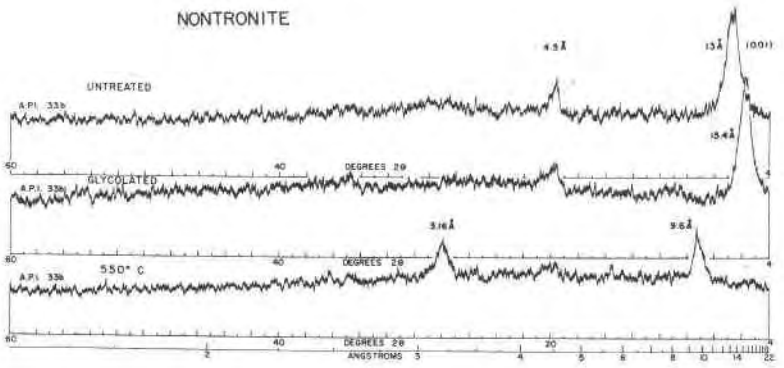

FIG. 4. *X*-ray diffractometer patterns for oriented A.P.I. nontronite.

coordinated will largely determine the position of (001) in the range 9.2–9.8 Å.

The problems introduced by mixed-layer structures in the diffractometer patterns of the group will be discussed under montmorillonite.

MONTMORILLONITE

The structural features of nontronite are characteristic for the entire montmorillonite group. *X*-ray diffractometer patterns of the untreated specimens (Fig. 5) show a few, diffuse reflections which are more intense than the corresponding peaks of nontronite. The most intense peak (Table VI) ranges in spacing from 12–15 Å, depending upon the number of water layers in the intersilicate position. The next more intense peak occurs at approximately 4.5 Å, and an asymmetric increase in background intensity is noted in the vicinity of 2.5 Å.

These three reflections persist in the glycolated patterns, with the characteristic expansion of (001) spacing. Diethylene glycol mono-

TABLE V. X-RAY DIFFRACTOMETER SPACING AND INTENSITY MEASUREMENTS FOR ORIENTED A. P. I. NONTRONITE

NONTRONITE									
Untreated						Glycolated		550° C.	
ASTM 2-0008[1]			A. P. I. 33b[2]						
(hkl)	dA	I_{REL}	dA	I_{ABS}	I_{REL}	dA	I_{ABS}	dA	I_{ABS}
(001)	15.4	100	13.1-13.5	63	100	15.4B	68	9.6	42
								5.70	28
	4.56	100	4.51	38	60	4.49-4.51	36	4.49B	29
			3.49	31	49			3.51	28
						3.29	33		
						3.18	31	3.16B	38
	3.11	20							
	3.03	20							
								2.84	27
	2.64	80							
	2.56	80				2.59B	33	2.57B	25
								2.47	25
	2.43	40							
	1.72	40	1.79	25	40			1.74	22
	1.67	40				1.69	27		

[1] Unoriented specimen; Nontron, Dordogne. Nagelschmidt, G., Min. Mag., 25, 140-155 (1938).

[2] Manito, Washington. B = broad.

butyl ether was employed in this study to expand the montmorillonite lattice. A number of organic molecules cause similar expansion, and MacEwan (1948) and others have described the organic complexes formed, and the expansion observed.

As in the case of nontronite (Fig. 4), upon heating to 550° C., montmorillonite collapses to an anhydrous spacing of about 9.6 Å for (001) and a pronounced reflection appears near 3.17 Å. The 4.5 Å spacing decreases slightly to about 4.42 Å, while the asymmetric peak near 2.5 Å remains unchanged.

The five montmorillonite patterns shown in Fig. 5 are somewhat complicated by the presence of several intense extraneous reflections. These are particularly noted in the patterns of A.P.I. 27. Five of the intense peaks in this pattern are caused by quartz ("Q"). The remaining reflections are best explained (Table VI) as caused by a mixed-layer structure of montmorillonite-chlorite ("M-C").

The montmorillonite species are particularly subject to the phenom-

enon of mixed-layer structure. The basic illite, chlorite, vermiculite, and montmorillonite structures are similar; the main distinction being in the composition of the intersilicate layer. Although the different compositions of this layer result in considerably different unit cell spacings in the *c* direction, the structures are often found interlayered in both random and regular patterns. The (001) series of reflections occur in an integral sequence in the regular mixed-layer clays, in distinction to the random mixed-layer structures. A new field has developed in the interpretation of mixed-layer clay structures (Earley *et al.*, 1956; Weaver, 1956, 1958).

Electron micrographs of montmorillonite samples show irregular flakes with only slightly more evidence of crystallinity than allophane. Hectorite, saponite, and nontronite may show lath-like forms, occasionally with striations parallel to their length, indicating cleavage resulting from

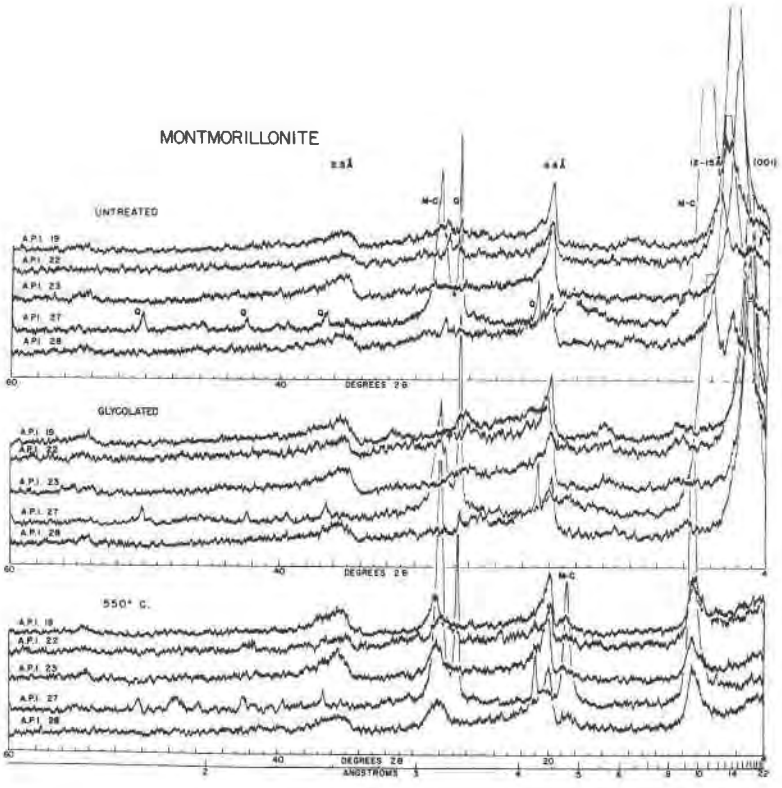

FIG. 5. *X*-ray diffractometer patterns of oriented A.P.I. montmorillonite. Impurity reflections are labeled: Q = quartz; M-C = montmorillonite-chlorite.

TABLE VI. X-RAY DIFFRACTOMETER SPACING AND INTENSITY MEASUREMENTS FOR ORIENTED A.P.I. MONTMORILLONITE

a. Untreated. b. Glycolated. c. 550° C.

a. Untreated

ASTM 3-0010[1]		A.P.I. 19[2]			A.P.I. 22[3]			A.P.I. 23[4]			A.P.I. 27[5]			A.P.I. 28[6]		
(hkl)	dA	I_{REL}	dA	I_{ABS}	I_{REL}	dA	I_{ABS}	I_{REL}	dA	I_{ABS}	I_{REL}	dA	I_{ABS}	I_{REL}	dA	I_{ABS}	I_{REL}
												22	48	23			
(001)	15.1	100	13.6	~200	100	12.5B	63	100	14.5	~115	100	13.6	~210	100	12.9B	~110	100
	5.1	40															
												4.8B	24	11			
	4.6	80	4.47B	34	17	4.46B	30	48	4.44	40	35	4.43	19	9	4.42B	33	30
	4.27	30										(4.26)	28	13	4.25	28	24
			3.34	20	10	3.33	24	38	3.38	18	16	(3.34)	82	39			
			3.23	20	10	3.24	25	40				3.21	45	21	3.19	24	22
												3.17	69	33			
	3.08	50				3.02	20	32	3.09	18	16						
			2.92	15	8				2.95	16	14						
	2.76	10															
	2.56	70	2.49-2.59	11	5	2.52-2.57	14	22	2.51-2.58	20	17	2.55	13	6	2.49-2.59	10	16
	2.50	40															
												2.47B	16	8			
												(2.28)	12	6			
	2.24	20							2.23	15	13	(2.23)	17	8			
									2.08	14	12	(2.12)	13	6			
												(1.81)	15	7			
	1.69	30							1.69	14	12	(1.68)	10	5			
									1.62	12	10						

b. Glycolated

A.P.I. 19[2]		A.P.I. 22[3]		A.P.I. 23[4]		A.P.I. 27[5]		A.P.I. 28[6]	
dA	I_{ABS}	dA	I_{ABS}	dA	I_{ABS}	dA	I_{ABS}	dA	I_{ABS}
16.6	~160	16.5	~150	16.7	98	16.3	80	17.4	~170
						13.5	87		
						10.8	~175		
		8.8	20					8.9-9.2	19
		8.35	19						
				7.03	13				
								6.48	15
5.49-5.62	14			5.57	15			5.86	16
4.45	32	4.42	34	4.41-4.49	32	4.45	20	4.48	35
				(4.26)	30				
		4.19	26						
		4.10	25	4.14	21				
						3.73	13		
								3.63	20
								3.56	21
		3.43	25	3.45B	19			3.45-3.50	20
3.33-3.41	20					(3.34)	84	3.35	22
		3.29	23						
		3.20B	22			3.21	35	3.21	16
						3.17	53		
		2.96	18					2.94	14
2.83	12								
2.50-2.58	17	2.52-2.59	20	2.52-2.60	17			2.49-2.59	17
2.48	15					2.46	14	2.44	15
						(2.28)	11	2.29	13
						(2.12)	11		
						(1.81)	13		
				1.70	10				
				1.68	11			1.69	12
1.69	11	1.69B	13	1.64	10				
						1.56	9		

c 550° C

A.P.I. 19[2]		A.P.I. 22[3]		A.P.I. 23[4]		A.P.I. 27[5]		A.P.I. 28[6]	
dA	I_{ABS}	dA	I_{ABS}	dA	I_{ABS}	dA	I_{ABS}	dA	I_{ABS}
						22*	21		
						12.0	21		
9.4-9.6	25	9.4-9.8	37	9.4-9.7	25	9.7	~145	9.4-9.7	34
						7.62	12		
						4.78*	55		
4.64	13								
4.42-4.45	18	4.40-4.50	27	4.42	34			4.44	34
				4.29	22				
						(4.26)	27		
		4.21	20	4.21	22			4.17	23
		3.77B	17						
		3.31	19			(3.34)	83		
		3.23	22						
3.11-3.16	20	3.17	23	3.10-3.20	23	3.19	~120	3.10-3.22	21
		3.00	16			2.97*	14		
2.41-2.59	15	2.42-2.60	15	2.51	20	2.47	15	2.45-2.68	15
				2.45-2.47	16				
						(2.28)	11		
		2.10-2.14	13			(2.11B)	12		
						1.99B	10		
						1.91-1.92	11		
						(1.81)	11		
1.68-1.69	9			1.69B	11				

1 Unoriented specimen; Algiers. Favejee, J. C. L., Z. Krist., 100, 433 (1939).
2 Polkville Mine; Polkville, Mississippi. B = broad.
3 Itawamba Mine, Amory, Mississippi.
4 Chambers, Arizona.
5 Belle Fourche, South Dakota. Quartz reflections are enclosed in parentheses.
6 Little Rock, Arkansas.
* Spacings similar to montmorillonite-chlorite heated to 550°C. Earley et al., Am. Mineral., 41, 262.

strains induced in the structure by differences in the ionic radii of octahedrally coordinated cations. Variation in the spacing and intensity of x-ray reflections similarly indicate differences among the montmorillonite minerals.

Illite

The term illite is applied to the mica-like clay mineral with a 10 Å c-axis spacing and a non-expanding lattice. Yoder and Eugster (1955) suggest the use of illite as a field term describing polymorphic forms of

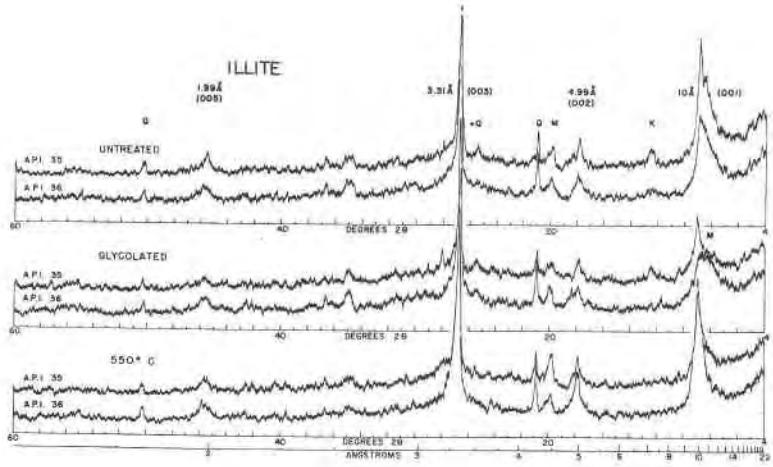

Fig. 6. X-ray diffractometer patterns for oriented A.P.I. illite. Impurity reflections are labeled: M = montmorillonite; Q = quartz; K = kaolinite.

mica, which may be interlayered with montmorillonite. The principal difference between illite and muscovite-sericite is in the degree of crystallinity which reflects the greater compositional range permitted in the illite lattice. X-ray diffractometer charts of illite show a few, broad, diffuse, weak reflections (Fig. 6), in contrast to the numerous sharp, strong peaks of muscovite and sericite (Table VII). Electron micrographs reveal the platy, irregular aggregates of illite, against the large, clean-cut plates of sericite and muscovite.

Except for a series of sharp quartz reflections, the x-ray diffractometer patterns of illite (Fig. 6) are characterized by several weak, broad peaks. These remain constant in spacing and intensity after glycolation. Heat treatment causes no shift in lattice spacing, but results in a slight increase in the peak intensities (Table VII).

The asymmetry of the 10.0 Å, (001) reflection probably indicates the presence of mixed-layer structures of montmorillonite-illite. Upon glycolation this reflection is reduced in intensity and in A.P.I. 36 shifts to slightly larger spacings. After heating to 550° C., the intensity is restored and the peak becomes symmetrical, indicating the collapse of the hydrated montmorillonite lattice to the anhydrous spacing, and a possible increased ordering of the illite lattice components.

Differential thermal analyses of these illite specimens (Kerr *et al.*, 1951) reveal a series of reactions upon heating, which may be attrib-

TABLE VII. X-RAY DIFFRACTOMETER SPACING AND INTENSITY MEASUREMENTS FOR ORIENTED A. P. I. ILLITE

	ILLITE																			
	Untreated										Glycolated				550° C.					
	MUSCOVITE ASTM 7-25[1]		ASTM 9-343[2]		A. P. I. 35[3]			A. P. I. 36[4]			A. P. I. 35[3]		A. P. I. 36[4]		A. P. I. 35[3]			A. P. I. 36[4]		
(hkl)	dA	I_{REL}	dA	I_{REL}	dA	I_{ABS}	I_{REL}	dA	I_{ABS}	I_{REL}	dA	I_{ABS}	dA	I_{ABS}	dA	I_{ABS}		dA	I_{ABS}	
					(10.48)	47	78				(16.5)	21								
(001)	10.08	100	10.0	100	10.0	60	100	10.0	42	100	10.0	34	10.0	31	10.0	46		10.0	61	
					(7.15B)	19	32				(7.12)	15								
(002)	5.04	37	4.95	20	4.98	33	38	4.98B	20	48	4.99	18	4.98	18	4.99	21		4.99B	25	
	4.49	90	4.48	90	4.47	20	53	4.47B	18	43	4.41-4.51	16	4.48	18	4.48	22		4.48	17	
	4.35	27																		
					(4.26)	26	43	(4.26)	27	64	(4.26)	21	(4.26)	27	(4.26)	23		(4.26)	28	
	4.11	16																		
	3.66	60	3.69	30	3.66	17	28													
					3.51	20	33				3.52	17			3.51	18				
					(3.34)	73	120	(3.34)	79	188	(3.34)	51	(3.34)	80	(3.34)	74		(3.34)	87	
(003)	3.36	100	3.33	90	∿3.30	28	47	∿3.30	30	71	∿3.30	23	∿3.29	32	∿3.29	26		∿3.30	32	
			3.17	5	3.19	22	37	3.21	22	52	3.18	21			3.19	20				
	3.07	50									3.07	16								
								(2.96-2.98)	16	38			(2.97)	16				(2.98)	15	
			2.87	10				2.88	16	38			2.89	15	2.90	14				
					2.84	16	27				2.84	14	(2.84)	15						
	2.689	16	2.61	60																
	2.582	50																		
	2.565	90	2.51	10	2.54-2.59	16	27	2.54-2.60	17	40	2.55-2.57	13	2.57B	16	2.55-2.57	14		2.55-2.59	12	
(004)	2.550	22																		
	2.450	11	2.42	40	2.45	16	27	2.45B	16	38			2.44	14	2.45	13		2.45	11	
	2.380	12						(2.28)	12	29								(2.28)	10	
	2.156	20	2.16	20				2.18	12	29								(2.11)	13	
(005)	2.013	32	1.986	10	1.99	17	28	1.99B	15	36	1.99B	10	1.99B	12	1.99B	13		2.00B	14	
					(1.81B)	13	22	(1.81)	12	29	(1.81)	9	(1.81)	9	(1.80B)	10		(1.81)	11	
	1.668	18	1.667	30	1.68	11	18	1.68	13	31										
											1.65-1.68	9								
	1.653	12			1.65	11	18													
	1.635	12			1.63	11	18				(1.61)	8								

[1] Synthetic 1M type; Yoder and Eugster, Geochim. et Cosmochim. Acta., 8, 225 (1955). Reflections with relative intensity less than 10 are not listed.
[2] Carden Wood, Aberdeenshire; Walker, G. F., Min. Mag., 29, 72-84 (1950).
[3] Fithian, Illinois. B = broad. Quartz, montmorillonite, and kaolinite reflections are enclosed in parentheses.
[4] Morris, Illinois. Quartz reflections are enclosed in parentheses.

uted to montmorillonite and kaolinite, with which illite is frequently interlayered. The diffractometer pattern of A.P.I. 35 indicates the presence of both of these minerals, while kaolinite is absent in A.P.I. 36.

The coincidence of the (003) reflection of illite with the 3.34 Å, most intense quartz peak, has resulted in certain problems. Although other reflections are present, quartz is often overlooked because of the masking of the most intense peak. Similarly, the precise spacing of the illite (003) reflection is difficult to determine because of the overlap of the intense quartz peak. Because of intensity ratios of the (001) and (003) muscovite peaks, and the asymmetrical small angstrom side of this reflection on the illite patterns, it is believed that the (003) reflection of illite approximates 3.30 Å, and these peaks are separately listed in Table VII.

Attapulgite

The clay-like mineral attapulgite is considered to be a finely crystalline relative of the palygorskite group.

A single intense reflection of 10.5 Å and a series of weak, broad lines at lesser angstrom spacings constitute the *x*-ray diffractometer pattern of attapulgite (Fig. 7). The intensities are slightly decreased and some peaks broadened by glycolation. Heating to 550° C. for two hours causes almost complete destruction of the pattern; the peaks which remain are primarily caused by montmorillonite and quartz (Table VIII).

The collapse of the attapulgite structure upon heating is a result first of the loss of H_2O and then of octahedrally coordinated OH ions. Dehydroxylation of the structure is almost complete at 550° C.

Unlike the other minerals examined in this study, attapulgite is not a sheet silicate structure. Bradley (1940) has described the mineral as a framework formed by the cross-linking of double-ribbed sheets. The double-ribbed effect represents the alternate pointing of the silica tetrahedra vertices to opposite sides of the "tetrahedral" layer. The channelways thus formed contain the H_2O molecules.

Electron micrographs reveal long straight fibers approximately 0.1×3 microns in width and length. Cleavage parallel to the ribs is considered responsible for the fiber-like habit.

Pyrophyllite

Pyrophyllite, the dioctahedral analogue of talc, was included in the original set of A.P.I. reference clays.

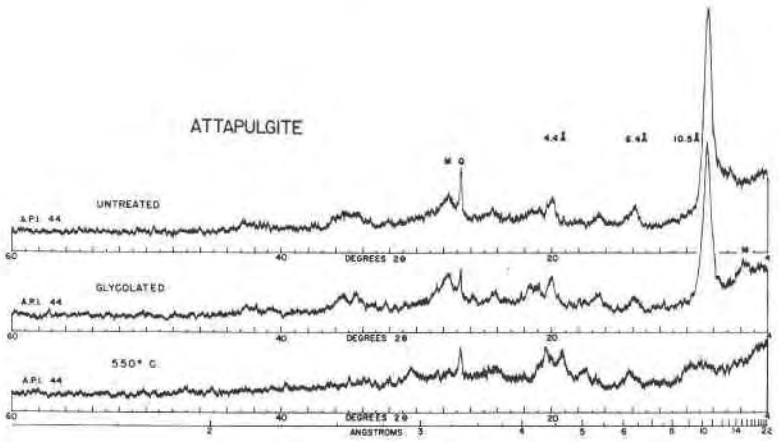

Fig. 7. *X*-ray diffractometer patterns of oriented A.P.I. attapulgite. Impurity reflections are labeled: Q=quartz; M=montmorillonite.

TABLE VIII. X-RAY DIFFRACTOMETER SPACING AND INTENSITY MEASUREMENTS FOR ORIENTED A. P. I. ATTAPULGITE

ATTAPULGITE									
Untreated						Glycolated		550° C.	
ASTM 5-0099[1]			A. P. I. 44[2]						
(hkl)	dA	I_{REL}	dA	I_{ABS}	I_{REL}	dA	I_{ABS}	dA	I_{ABS}
			(13.1)	33	36	(16B)	28		
(110)	10.50	100	10.5	91	100	10.5	72		
								(9.6B)	20
(200)	6.44	60	6.42B	18	20	6.43B	14		
								6.23	17
(130)	5.42	40	5.32-5.49	15	16	5.44	15		
						5.35	14	4.95-5.12	17
			4.65	14	15	4.65	14	(4.62B)	24
(040)	4.49	80	4.45B	20	22	4.48	22		
								4.34	25
			(4.26)	17	19	(4.26)	19	(4.26)	20
(310)	4.18	20	4.14	17	19	4.14B	19		
(240)	3.69	40	3.67	17	19	3.67-3.71	16		
(330)	3.50	20	3.48	15	16	3.49	15		
			(3.34)	32	35	(3.34)	24	(3.34)	25
(400)	3.23	100	3.22	23	25	3.21B	22		
						3.13	19		
(420)	3.03	10				3.04	14		
								(2.94)	18
			2.80	13	14	2.79	12		
			2.69	14	15				
(440)	2.61	80				2.61B	15		
			2.50-2.63	16	18			(2.57)	14
(510)	2.55	20				2.51-2.55	15		
			(2.46)	14	15				
			2.40	11	12				
			2.39	12	13	2.39B	9		
(530)	2.38	20	2.38	11	12				
(600)	2.15	40	2.14	12	13	2.15	11		
			(2.13)	11	12	(2.12B)	11		
			2.10B	12	13				
(390)	1.82	10	1.82	10	11	1.82	8		
(800)	1.62	10				1.62	9		

[1] Unoriented specimen; Attapulgus, Georgia. Bradley, W. F., Am. Mineral., 25, 405-410 (1940).

[2] Attapulgus, Georgia. Quartz and montmorillonite reflections are enclosed in parentheses. B = broad.

The sharp, intense reflections seen in the *x*-ray diffractometer patterns (Fig. 8) indicate excellent crystallinity, but only a few of the reflections are caused by pyrophyllite. The majority of the peaks represent well crystallized impurities including quartz, muscovite, and kaolinite or dickite (Table VIII), which comprise about 30 per cent of this specimen.

The diffraction pattern of pyrophyllite is unaffected by glycolation, and only slightly intensified by heating to 550° C. Dehydration is not noted, while dehydroxylation of the mineral has only begun at this

temperature and is not complete until above 780° C. Similarly, the low base exchange and isomorphous replacement reported for pyrophyllite explain the lack of response to glycolation.

Additional reflections have been noted in the pyrophyllite pattern by Gruner (Table IX) and others. Most are masked by the numerous impurity peaks, but the 4.15 Å spacing is absent. Otherwise, comparison of the A.P.I. with the A.S.T.M. pyrophyllite pattern is satisfactory.

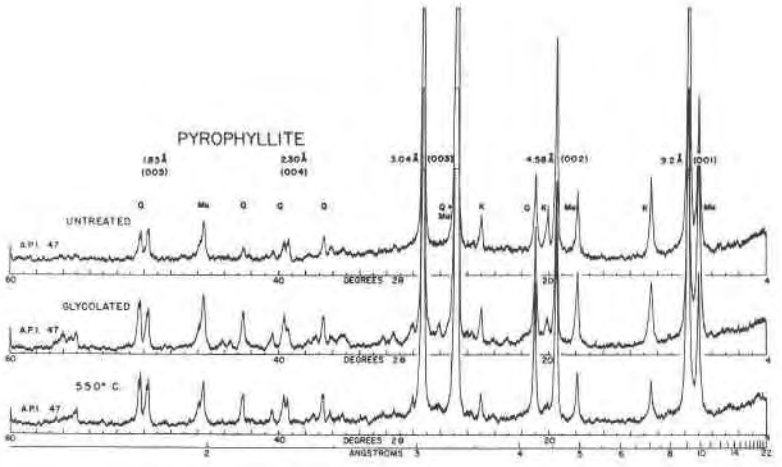

FIG. 8. *X*-ray diffractometer patterns of oriented A.P.I. pyrophyllite. Impurity reflections are labeled: Mu = muscovite; K = kaolinite or dickite; Q = quartz.

The isomorphism of talc and pyrophyllite structures, one dioctahedral, the other trioctahedral, presents difficulties in the distinction of these minerals. The main *x*-ray diffraction differences are the absence of the strong 3.13 and 2.62 Å talc spacings in the pyrophyllite pattern.

CONCLUSION

X-ray diffractometer techniques furnish an effective method for identifying and differentiating the clay minerals. Data for reference clay minerals from other forms of analysis are supplemented by diffractometer patterns and spacing-intensity measurements on the original chemically analyzed specimens of A.P.I. Research Project 49. Clay lattice spacing shifts and reactions observed in these *x*-ray charts are understandable in terms of changes within the clay mineral structure.

In conclusion, a schematic chart of diffractometer patterns (Fig. 9) is given for the clay minerals described. Extraneous lines have been re-

TABLE IX. X-RAY DIFFRACTOMETER SPACING AND INTENSITY MEASUREMENTS FOR ORIENTED A. P. I. PYROPHYLLITE

PYROPHYLLITE									
Untreated						Glycolated		550° C.	
ASTM 2-0613[1]			A. P. I. 47[2]						
(hkl)	dA	I_{REL}	dA	I_{ABS}	I_{REL}	dA	I_{ABS}	dA	I_{ABS}
			(10.0)	67	48	(10.0)	76	(10.0)	59
(001)	9.14	40	9.2	∿140	100	9.2	∿110	9.2	∿150
			(7.16)	37	26	(7.16)	28	(7.16)	20
			(5.01)	32	23	(5.00)	31	(4.98)	24
(002)	4.57	50	4.58	89	64	4.59	65	4.57	88
			(4.47)	26	19	(4.47)	14	(4.47)	12
			(4.26)	38	27	(4.26)	48	(4.26)	57
	4.15	20							
	3.87	5	3.87	11	8	3.87	7		
						(3.72)	7		
			(3.59)	23	16	(3.59)	18	(3.57)	15
						(3.49B)	13	(3.48B)	12
	3.34	20-40	(3.34)	∿150	100	(3.34)	∿140	(3.34)	55
						(3.19)	13		
(003)	3.04	100	3.04	∿140	100	3.04	∿125	3.04	∿150
						(2.98)	12		
			(2.87)	12	9	(2.87)	9	(2.86)	10
			(2.78B)	10	6	(2.79B)	7	(2.79)	9
			(2.56B)	11	8	(2.57B)	8		
	2.52	20	(2.50)	11	8	(2.51)	7	(2.51)	7
			(2.46)	15	11	(2.45)	15	(2.45)	15
	2.40	40	(2.39)	9	6			(2.40B)	8
(004)	2.29	20	2.30	14	10	2.30B	10	2.30	10
			(2.28)	13	9	(2.29)	16	(2.28)	15
			(2.23)	9	6	(2.24)	8	(2.23)	9
	2.14	10-20	(2.14)	8	5				
			(2.13)	10	7	(2.12)	16	(2.12B)	15
	2.07	10				(2.07)	6		
	2.04	10						(2.01)	20
			(2.00)	20	14	(2.00)	23	(2.00)	12
			(1.98)	12	9	(1.99)	12		
	1.88	5				(1.89)	4		
								1.86B	21
(005)	1.83	40	1.83	18	13	1.83	18		
			(1.81)	17	12	(1.82)	21	(1.82B)	24
			(1.68B)	8	5	(1.68)	9	(1.69B)	10
						(1.67)	9		
	1.64	20-40							

[1] Unoriented specimen; Tres Ceritos, Mariposa County, California. Gruner, J. W., Z. Krist., 88, 415 (1934).

[2] Processed; Robbins, North Carolina. Reflections primarily caused by quartz, muscovite, and kaolinite are enclosed in parentheses.

moved, the symmetry or asymmetry of each peak is imitated, and the intensities are absolute in terms of the equipment used. The corresponding chemical composition of the minerals is based on the analyses of A.P.I. Research Project 49. Dotted lines indicate the approximate level of background radiation in the charts.

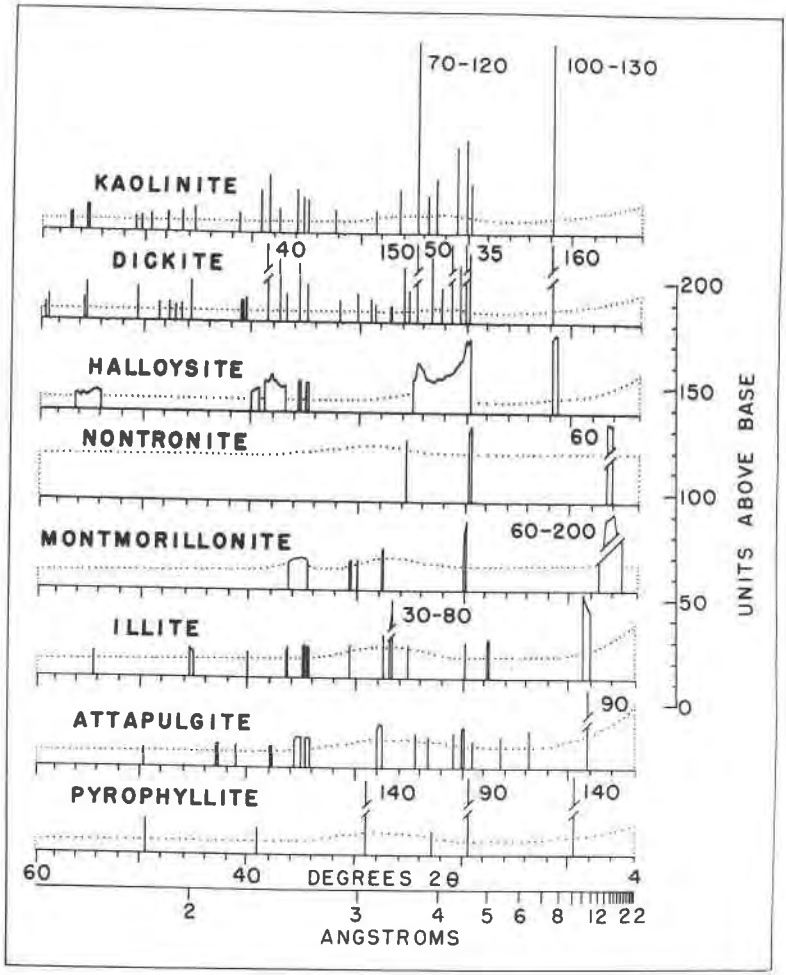

FIG. 9. Schematic diagram of A.P.I. diffractometer patterns. Intensity, spacing, width and symmetry of the principal reflections are imitated. Intensity is measured in units above base. The dotted line indicates the background level.

REFERENCES

BATES, T. F., HILDEBRAND, F. A., AND SWINEFORD, A., 1950, "Morphology and Structure of Endellite and Halloysite," *Amer. Mineral.*, **35,** 463–484.

BRADLEY, W. F., 1940, "The Structural Scheme of Attapulgite," *ibid.*, **25,** 405–410.

BRINDLEY, G. W., ed., 1951. *X-ray Identification and Structure of the Clay Minerals.* Mineralog. Soc. Gr. Brit., Monogr., 345 p.

———, AND ROBINSON, H., 1946, "Randomness in the Structures of Kaolinitic Clay Minerals," *Trans. Faraday Soc.*, **42B,** 198–205.

EARLEY, J. W., BRINDLEY, G. W., MCVEAGH, W. J., AND VANDEN HEUVEL, R. C., 1956, "A Regularly Interstratified Montmorillonite-chlorite," *Amer. Mineral.*, **41,** 258–267.

GRIM, R. E., 1953, *Clay Mineralogy,* 384 p. McGraw-Hill Book Co., New York.

GRUNER, J. W., 1932, "Crystal Structure of Dickite," *Z. Krist.*, **83,** 394–404.

HENDRICKS, S. B., 1938a, "On the Structure of the Clay Minerals: Dickite, Halloysite, and Hydrated Halloysite," *Amer. Mineral.*, **23,** 295–301.

———, 1938b, "Crystal Structure of Nacrite and the Polymorphism of the Kaolin Minerals," *Z. Krist.*, **100,** 509–518.

KERR, P. F., *et al.*, 1951, "Preliminary Reports, Reference Clay Minerals," *Amer. Petrol. Inst.*, Research Project **49**.

KSANDA, C. J., AND BARTH, T. F. W., 1935, "Note on the Structure of Dickite and Other Clay Minerals," *Amer. Mineral.*, **20,** 631–637.

MACEWAN, D. M. C., 1948, "Complexes of Clays with Organic Compounds, I," *Trans. Faraday Soc.*, **44,** 349–367.

MACKENZIE, R. C., ed., 1957, *The Differential Thermal Analysis of Clays.* 456 p. Mineralog. Soc., Clay Minerals Group, London.

MURRAY, H. H., AND LYONS, S. C., 1956, "Correlation of Paper-coating Quality with Degree of Crystal Perfection of Kaolinite," *Clays and Clay Minerals;* Proc. 4th Nat. Conf. on Clays and Clay Minerals; Publ. 456, Nat. Acad. of Sci., Nat. Research Council.

RAMSDELL, L. S., 1947, "Studies on Silicon Carbide," *Amer. Mineral.*, **32,** 64–82.

ROSS, C. S., AND KERR, P. F., 1931, "The Kaolin Minerals," *U. S. Geol. Survey Prof. Paper* 165E.

WEAVER, C. E., 1956, "The Distribution and Identification of Mixed-layer Clays in Sedimentary Rocks," *Amer. Mineral.*, **41,** 202–221.

———, 1958, "Geologic Interpretation of Argillaceous Sediments," *Bull. Amer. Assoc. Petrol. Geol.*, **42,** No. 2, 254–309.

YODER, H. S., AND EUGSTER, H. P., 1955, "Synthetic and Natural Muscovites," *Geoch. Cosmoch. Acta,* **8,** 225–280.

Manuscript received July 15, 1960.